2018

Radiation therapy for deep periocular cancer treatments when protons are unavailable: Is combining electrons and orthovoltage therapy beneficial?

Kevin Martell
University of Calgary

Yannick Poirier
University of Maryland

Tiezhi Zhang
Washington University School of Medicine in St. Louis

Alana Hudson
University of Calgary

David Spencer
University of Calgary

See next page for additional authors

Journal of Radiation Research, Vol. 59, No. 5, 2018, pp. 593–603
doi: 10.1093/jrr/rry045
Advance Access Publication: 25 June 2018

Radiation therapy for deep periocular cancer treatments when protons are unavailable: is combining electrons and orthovoltage therapy beneficial?

Kevin Martell[1,2,*,‡], Yannick Poirier[3,‡], Tiezhi Zhang[4], Alana Hudson[1,2], David Spencer[1,2], Ferenc Jacso[1,2], Richard Hayashi[2], Robyn Banerjee[1,2], Rao Khan[4], Nathan Wolfe[2] and Jon-Paul Voroney[1,2,†]

[1]Department of Oncology, University of Calgary, Tom Baker Cancer Centre 1331 29 Street Northwest, Calgary T2N 4N2, Alberta, Canada
[2]Calgary Zone, Alberta Health Services, Foothills Medical Centre, 1331-29 ST NW, Calgary, Alberta, Canada
[3]Department of Radiation Oncology, University of Maryland, 22 S Greene St, Baltimore, MD 21201, USA
[4]Department of Radiation Oncology, Washington University in St. Louis, 660 S. Euclid Ave., CB 8224, St. Louis, MO 63110, USA
*Corresponding author. Division of Radiation Oncology, University of Calgary, Tom Baker Cancer Centre 1331 29 Street Northwest, Calgary T2N 4N2, Alberta, Canada. Tel: +1-403-521-3378; Fax: +1-403-283-1651; Email: kevin.martell@albertahealthservices.ca
[†]Deceased
[‡]Contributions from these authors were equal and they should be considered as co-first authors.
(Received 21 October 2017; revised 31 January 2018; editorial decision 3 May 2018)

ABSTRACT

Deep periocular cancers can be difficult to plan and treat with radiation, given the difficulties in apposing bolus to skin, and the proximity to the retina and other optic structures. We sought to compare the combination of electrons and orthovoltage therapy (OBE) with existing modalities for these lesions. Four cases—a retro-orbital melanoma (Case 1) and basal cell carcinomas, extending across the eyelid (Case 2) or along the medial canthus (Cases 3–4)—were selected for comparison. In each case, radiotherapy plans for electron only, 70% electron and 30% orthovoltage (OBE), volumetric-modulated arc therapy (VMAT), conformal arc, and protons were compared. Dose–volume histograms for planning target volume coverage and selected organs at risk (OARs) were then calculated. The $V_{90\%}$ coverage of the planning target volume was >98% for electrons, VMAT, conformal arc and proton plans and 90.2% and 89.5% in OBE plans for Cases 2 and 3, respectively. The retinal $V_{80\%}$ was >98% in electron, VMAT and proton plans and 79.4%; and 87.1% in OBE and conformal arcs for Case 2 and 91.3%, 36.4%, 56.9%, 52.4% and 43.7% for Case 3 in electrons, OBE, VMAT, conformal arc and proton plans, respectively. Protons provided superior coverage, homogeneity and OAR sparing, compared with all other modalities. However, given its simplicity and widespread availability, OBE is a potential alternative treatment option for moderately deep lesions where bolus placement is difficult.

Keywords: orthovoltage; electrons; periocular; periorbital; planning; radiation

INTRODUCTION

Periocular malignancies, particularly skin cancers, are difficult to treat due to the sensitive location of the tumor with regards to organs at risk (OARs) such as the retina, lens, and optical nerve. Traditionally, orthovoltage photon therapy or electron treatments are used to treat superficial lesions; however, due to the challenging anatomy, neither technique currently provides the oncologist with optimal dose distributions for tumor coverage and eye sparing. Whereas orthovoltage treatments are inadequate for treating deeper tumors but provide an excellent opportunity for shielding the eye

due to sharp radiation penumbras, electron beams produce out-of-field scatter, which deposits more dose in the retina or lens, and they are challenging to shield [1, 2]. In these cases, bolus (e.g. of wax or Superflab Bolus Material) can extend the dose coverage to the skin surface, but results in large treatment volumes, poorly reproducible set-up and decreased dose at depth, while tantalum mesh maintains dose at depth but causes inhomogeneities [1, 3].

Recent therapy developments include use of IMRT techniques [e.g. volumetric-modulated arc therapy (VMAT)], proton therapy and brachytherapy [4–8]. However, these treatments have associated costs and require specialized support staff and experience [8–10]. While attractive due to their Bragg peak, protons remain unavailable to many centers, particularly in Canada and Australia. IMRT and brachytherapy are more widely available, but IMRT is associated with a high out-of-field dose due to the many beam projections involved, while penetration suffers in brachytherapy due to inverse-square drop-off. Because of this, alternative treatments such as oculoplastic surgery, Moh's micrographic surgery or radiotherapy with plan for salvage enucleation are often used [11].

We propose a combination of megavoltage (MV) electron radiotherapy and orthovoltage/kilovoltage (kV) X-rays to optimize treatment both at depth and at the skin surface. The objective of this study was to describe this novel technique, its rationale and its clinical set-up, and to provide proof-of-concept by comparing dose distribution with other modalities in four potential clinical cases: OBE, electrons alone, VMAT plans using coplanar beams, non-coplanar dynamic arc therapy, and protons.

Historically, kilovoltage X-ray therapy has not been used to its potential. This is partly due to technical limitations in computing dose distributions, which means that dose distributions are very rarely (if ever) assessed in orthovoltage radiotherapy [12, 13]. In this study, we use the recently developed and thoroughly validated kilovolt X-ray dose calculation algorithm kVDoseCalc to calculate patient-specific kilovolt dose distributions [14–19]. While our study is based on a limited four cases, we have established the potential of this novel technique for offering a cheaper, more convenient alternative to protons in treating periocular tumors.

MATERIALS AND METHODS

Proposed technique rationale

Both orthovoltage X-ray and electron therapy have long been used in treating surface and near-surface tumors. However, each technique has limitations regarding potential in treating periocular tumors.

Electrons benefit from a finite range, which can limit the dose to deep OARs such as the optical nerve. However, the presence of a build-up region leads to a low surface dose, particularly at lower energies and wide penumbras. While the surface dose can be increased by the placement of bolus, this reduces the range of the electrons in the tissue, necessitating the use of a higher electron energy and, consequently, even wider penumbras.

In contrast, secondary charged particles released by orthovoltage X-rays have submillimeter range. Consequently, they show no build-up region (i.e. high surface dose) and sharp penumbras, which allow for geometric sparing of OARs. However, their lower energy increases attenuation and the influence of the photoelectric effect; therefore, dose fall-off is faster than with megavolt photons, and they can deposit up to approximately four times more dose in bone.

We propose combining electron and orthovoltage therapy to maximize the advantages and mitigate the disadvantages of these two techniques. When using a cleverly weighted sum consisting of 70% 9 or 12 MeV electrons + 30% 200 kVp photons, a combined dose distribution is produced in which the kilovolt photon fall-off is almost perfectly compensated for by build-up in the electron beam, such that the percentage depth dose (PDD) is nearly flat (<1% variation) within the first 4 cm. Furthermore, the combined beam has a tighter penumbra compared with the electron beam, potentially allowing for geometric sparing of the OAR. Figure 1 shows the

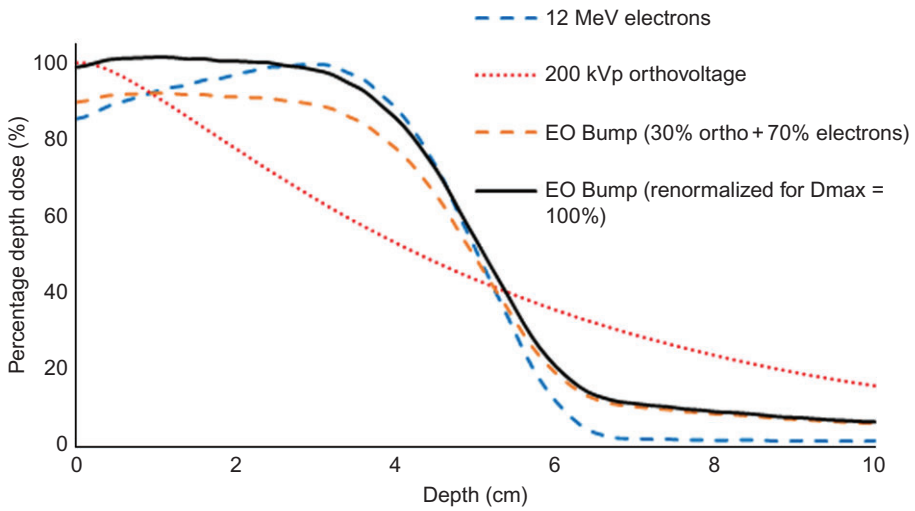

Fig. 1. Percentage depth–dose profile for 12 MeV electrons (broken blue line), 200 kVp orthovoltage photons (red dotted line), EO Bump (broken orange line) and EO Bump renormalized to 100% dose (black).

Fig. 2. Set-up for combination electrons with orthovoltage bump cases. Top: electron portion of treatment. Patients are immobilized within an Aquaplast shell; orbital shielding (only in medial canthus cases) is provided directly in the aperture. Bottom: orthovoltage therapy is performed with a tungsten eye shield in place and a custom lead cut-out.

central axis PDD for a $6 \times 6\,cm^2$ 12 MeV electron beam, and a 6 cm 200 kVp orthovoltage beam at 30 cm focal-to-surface distance (FSD). The cross-sectional profile can be seen in Supplementary Fig. 1.

Since they are delivered independently on different treatment units, the electron and orthovoltage components of the OBE technique are independently prescribed at d_{max} (for electrons) and surface (for orthovoltage). However, the OBE PDD has a nominal maximum value of 90%, thus a normalization by 1.1 to bring d_{max} to 100% is necessary. In practice, since the dose at the edges of the field is lower than at the CAX due to scatter and penumbra, the OBE was prescribed to bring d_{max} to 107% of the prescribed dose, with the intent to keep the planning target volume (PTV) dose between 95 and 107%.

Patient cases

We identified four patients presenting periorbital malignancies treated between December 2013 and December 2016. Patient 1 had a pathologically proven retro-orbital melanoma and refused enucleation (Case 1). Case 2 was a basal cell carcinoma of the right orbit with destruction of the upper lid and extension to the frontal bone. Cases 3 and 4 were basal cell carcinomas of the medial canthus abutting the globe and extending along the lid to different extents. Patients 1 and 3 were treated with conformal arc therapy, Patient 2 with electrons, and Patient 4 with OBE. For each patient, retrospective radiation therapy plans were created for each modality using their original simulation CT and structure set. The Health Research Ethics Board of Alberta reviewed the protocol and found that the research qualified as a quality assurance/improvement review and did not require a formal research ethics review [20]. In the case of patient set-up being presented, written consent was obtained to use photographs.

Set-up

Each patient in this study had previously undergone CT simulation scanning with an Aquaplast® shell (Aquaplast Corp, Avondale USA) immobilization mask with external metal ball bearing (BB) markers for laser localization. Passive eye immobilization involved directed gaze to a pin-hole. For cases treated with non-coplanar arcs or VMAT, institutional standards of practice were adhered to and prescription doses were between 4000 cGy in 10 fractions and 5000 cGy in 20 fractions at the discretion of the treating physician. For the case treated with OBE (Case 4) and the case treated with electrons (Case 2), the prescribed dose was similar when the radiobiologic effective dose was taken into consideration. With set-ups as shown in Fig. 2, the orthovoltage bump patient first received electron therapy for 7 out of 10 scheduled fractions. No bolus was used in these treatments, and patients were immobilized in an Aquaplast® shell (Aquaplast Corp, Avondale USA) that was cut out around the affected eye. During electron treatment, a small tungsten shield was placed directly in the electron applicator and held in place using a magnet, such that the patients' globes were not receiving the primary dose from the electron beam. Position was optimized using the Linac light field. The remaining three fractions of radiation were delivered using 200 kVp orthovoltage therapy and a custom lead cut-out with a tungsten internal eye shield.

Contouring

All patients were contoured by the same physician according to guidelines described by Brouwer *et al.* [14]. For all patients, additional structures included the eyelid and the retina, defined as a 2 mm internal contour of the eye contour excluding the anterior chamber. Gross tumor volume (GTV) structures were contoured by the treating physician and confirmed by a second coauthor in all cases. The clinical tumor volume (CTV) was defined as a 1 cm symmetric expansion about the GTV and cropped to normal uninvolved bone and globe. The PTV was a symmetric 3 mm expansion about the CTV in all cases. Example contours for each of these are found in Supplementary Fig. 2. For VMAT, planning optimization structures were made as follows: VMAT_PTV 1 mm symmetric expansion about the PTV, PTV plus retina, PTV minus retina, and retina outside of PTV.

Because of limitations in the CT planning software with shield modeling, an additional evaluatory PTV (PTVEval) was created for OBE calculations when applicable. This structure consisted of the original PTV trimmed to a line parallel to the field and perpendicular to the position of the eye shield to provide adequate modeling of the same (Supplementary Fig. 3) [15]. This was of particular importance in Case 2, where the gross tumor involved the eyelid

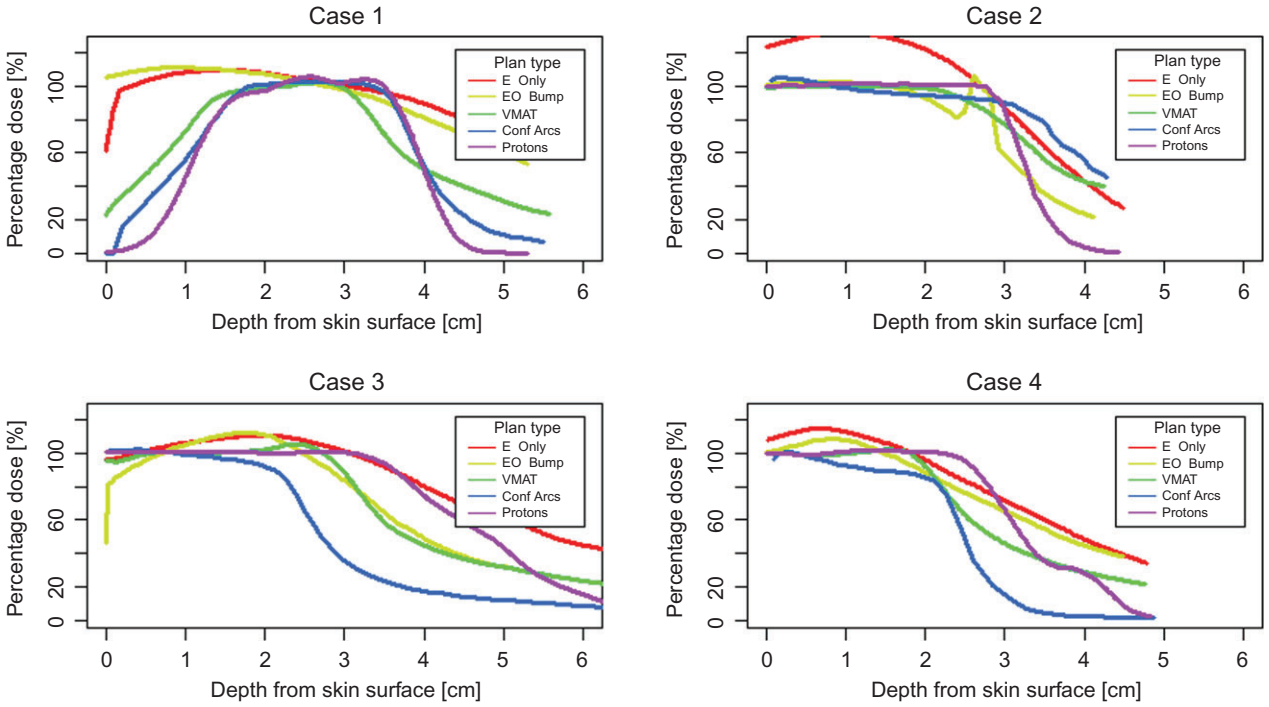

Fig. 3. PDD profiles by modality. Plotted are percentage depth–dose profiles for Case 1: retro-orbital melanoma; Case 2: large squamous cell carcinoma over superior eyelid; Case 3: medial canthus lesion number 1; and Case 4: second medial canthus lesion. Red, orange, green, blue and magenta colors correspond to plans for electron therapy, electrons with orthovoltage bump, volumetric-modulated arc therapy, conformal arc therapy and proton therapy, respectively.

and would be treated in practice, but there would be little dose below the eyelid due to shielding. In subsequent dose–volume histogram (DVH) calculations, this PTV was used and compared with the PTVs as described above for all other plans.

Dosimetric calculations

Proton plans were generated in a proton therapy facility by an expert planner using the Aria Eclipse™ version 13.6.14 for a 250 MeV dual-scattering MeVion synchrocyclotron therapy device [16]. Non-coplanar conformal arc treatments were planned using iPlan (Brainlab Inc, Feldkirchen, Germany). VMAT plans were planned using Aria Eclipse™ (Varian Medical Systems Inc, Palo Alto, USA) using the AAA algorithm, while electron plans (for electrons alone or as part of the OBE) used the electron Macro Monte Carlo (eMC) dose calculation algorithm. Case 1 was planned using 16 MeV electrons due to lesion depth, while Cases 2–4 were planned with 12 MeV electrons. For electrons alone, the plans were normalized to a PTV coverage of $V_{95\%} = 95\%$. The orthovoltage component of OBE plans were created using our kilovolt X-ray dose calculation software, kVDoseCalc for a Xstrahl 300 orthovoltage unit using a 200 kVp 30 cm FSD beam developed at our institution [17]. This software was previously used to characterize this X-ray beam and has been extensively validated for superficial kilovolt dose calculation applications [18, 19, 21, 22]. The field aperture was created using the electron beam's eye view of the PTVEval structure to simulate a surface cut-out. The two dose distributions were then superimposed using weighting of 70% electron dose profile and 30% orthovoltage dose profile to generate the final dose distribution. All final OBE dose distributions were renormalized to a maximum dose of 107%.

The tungsten eye shield was not modeled, as the kVDoseCalc software does not currently support structure-based Hounsfield unit (HU) overrides. Since tungsten is a high atomic number ($Z = 74$) material, 1 mm is sufficient to attenuate >98% of the beam [23]. Therefore, we modeled the effect of the tungsten shield by restricting the orthovoltage beam aperture to where the eye was not shielded. Bolus was created for cases and modalities where it was clinically indicated (e.g. VMAT) and assigned a HU of 0. Contouring and planning were performed by a single physician–planner pair to ensure uniformity in planning practices. All plans were then reviewed by a second physician and planner, as is done in quality assurance rounds.

Data analysis

PDD profiles were calculated along a user-defined line perpendicular to and starting at body surface (i.e. bolus excluded), going through the GTV and aligned with the central axis of the electron or orthovoltage beam. In each case, between modalities, the same coordinates were used to calculate PDD profiles. Although it is not necessarily applicable for comparative purposes, the same depth–dose profiles using the same start and end points were generated for VMAT and conformal arc plans. We reported depths (in

Table 1. Depth–dose values

Case number	Modality	Dose at 1 mm [%]	d_{max} [cm]	$De_{90\%}$ [cm]	$De_{30\%}$ [cm]
Case 1	Electrons	87.0	1.5	4.0	>5.3
	OBE	106.3	1.0	3.5	>5.3
	VMAT	29.4	2.7	3.2	5.1
	Conformal arcs	0.1	2.9	3.6	4.3
	Proton plans	0.9	2.6	3.7	4.2
Case 2	Electrons	125.0	1.0	2.9	4.4
	OBE	101.2	2.6	2.8	3.7
	VMAT	99.5	1.5	2.6	>4.3
	Conformal arcs	104.3	0.2	3.0	>4.3
	Proton plans	100.2	1.1	2.9	3.4
Case 3	Electrons	96.7	1.9	3.6	7.4
	OBE	83.7	1.8	2.8	5.1
	VMAT	95.0	2.4	3.0	5.2
	Conformal arcs	101.4	0.4	2.1	3.2
	Proton plans	100.7	1.0	3.6	5.3
Case 4	Electrons	109.1	0.8	2.2	4.8
	OBE	101.4	0.9	1.9	4.5
	VMAT	100.0	1.5	2.1	3.9
	Conformal arcs	96.7	0.3	1.3	2.6
	Proton plans	100.2	1.3	2.6	3.9

Values of $De_{x\%}$ are the depth at which the *x*% isodose line occurs along the central axis of the beam (i.e. $De_{90\%}$ is the depth at which the 90% isodose level is encountered).

centimeters) at which the maximum dose (d_{max}) and the 90% isodose level ($De_{90\%}$) were encountered. Additionally, $De_{30\%}$ and the dose at 1 mm were calculated. We also reported DVHs for the PTV (specifically $V_{90\%}$) and OARs for each case and modality. Finally, axial slices aligned with the central axis of the beam are shown with calculated dose distributions. All data analyses were performed using the R programming language version 3.1.1 (www.r-project.org).

RESULTS

Depth–dose profiles

Depth–dose profiles for protons, electrons only and OBE plans are shown in Fig. 3 for each of the four cases. Comparing electrons plus bolus with OBE plans, d_{max}, as expected, was similar when calculated as depth from skin surface (Table 1). With proton therapy plans, $De_{30\%}$ was shallower in Cases 1, 2 and 4. In Case 3, conformal arc therapy had the lowest $De_{30\%}$ (3.2 cm). As seen in Fig. 3, there was also less heterogeneity in dose for the proton plans when compared with other modalities.

Isodose distributions

As shown in Fig. 4, the lateral dose washout was most pronounced in the VMAT plans, followed by electron-only treatments. However, with plan optimization, most 30% isodose levels were limited to small volumes of the brain, and the contralateral orbit was universally spared. As expected, conformal arc therapy and proton therapy plans showed very steep dose gradients with exceptional sparing of normal tissues. Reassuringly, OBE plans showed similar normal tissue sparing in Cases 3 and 4.

Dose–volume histograms

Cumulative DVHs for PTV coverage across modalities are presented in Fig. 5. In Case 2, the electron treatment required a high

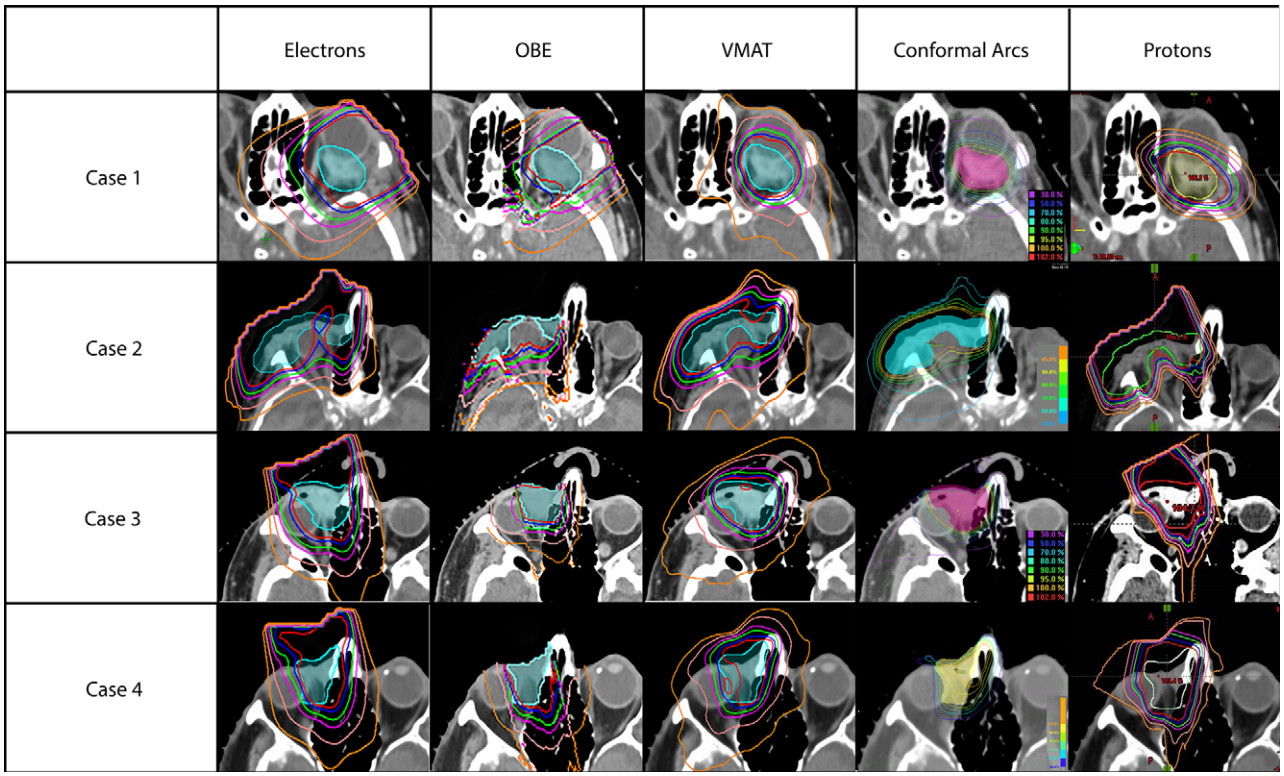

Fig. 4. Isodose distributions for each case for electrons only, electrons with orthovoltage bump, volumetric-modulated arc therapy, conformal arc plans and proton therapy plans. Unless otherwise indicated, red, blue, green, magenta, beige and orange correspond to 95%, 90%, 80%, 70%, 50% and 30% isodose levels, respectively. Differences noted in image resolution are due to display differences between planning systems. OBE: electrons with orthovoltage bump; VMAT: volumetric-modulated arc therapy.

normalization to ensure $V_{95\%} > 95\%$; therefore, a hotspot of 120% is present. In OBE cases, orthovoltage X-rays deposit 3–4 times as much dose in bone as in tissue due to the photo-electric effect, causing hot spots of up to 175% where bone overlaps with the PTV. Consequently, in all OBE cases, ~10% of the volume received 120% of the prescribed dose due to the varying presence of bone in the PTV.

In Table 2, we compared the following metrics between techniques for all four cases: target coverage in terms of $V_{90\%}$ and $V_{95\%}$ in the PTV, $V_{80\%}$ in the ipsilateral retina, and $V_{100\%}$ in the ipsilateral optic nerve. For the ipsilateral retina, $V_{80\%}$ (40 Gy) represents an equivalent dose in 2 Gy fractions (EQD2 Gy) of 44 Gy, which has been associated with morbidity [24]. Similarly, $V_{100\%}$ corresponds to an OAR dose $< d_{max}$ (50 Gy/20 fx, EQD2 Gy 3 = 55 Gy) for the ipsilateral optical nerve. Cumulative DVH plots for the ipsilateral retina and optic nerves are shown in Figs 6 and 7.

DISCUSSION

We present a comprehensive comparison of dosimetry between OBE, EO, VMAT, conformal arc, and protons, with DVH distributions for each.

Each technique offers advantages and disadvantages. In terms of sharp penumbras and geometric sparing, electrons and VMAT performed the worst, followed by conformal arcs, while protons and the OBE technique performed the best. On the other hand, in terms of conformality, electrons and OBE performed the worst.

For Cases 1 and 2, the OBE technique was completely unsuitable and would have led to undesirable dose distributions. In Case 1, the target was too deep (OBE is only a good technique when using 12 MeV electrons for a treatment depth of ≤4 cm). In Case 2, the extensive disease did not permit geometric sparing of OARs, so more conformal techniques, such as protons, VMAT, or conformal arcs, produced superior dose distributions. This is seen in the DVH metrics (Table 1).

However, in Cases 3 and 4, the OBE technique achieved the best geometric sparing of the ipsilateral retina and optical nerve. In Case 4, the coverage metrics (PTV $V_{90\%}$, $V_{95\%}$) were similar to those achieved by the other techniques. In principle, the DVH metrics for Case 3 showed inferior coverage ($V_{90\%}$ and $V_{95\%}$ of 89.5% and 73.1%, respectively) to the OBE technique. However, this was caused by the PTV expanding the target beyond the ≤4 cm therapeutic range of the technique. In fact, the corresponding $V_{90\%}$ and $V_{95\%}$ for the GTV were 99.9% and 95%, respectively. This was partly caused by the fact that we used an identical PTV expansion (3 mm isotropic) for all techniques. However, when using a single-field

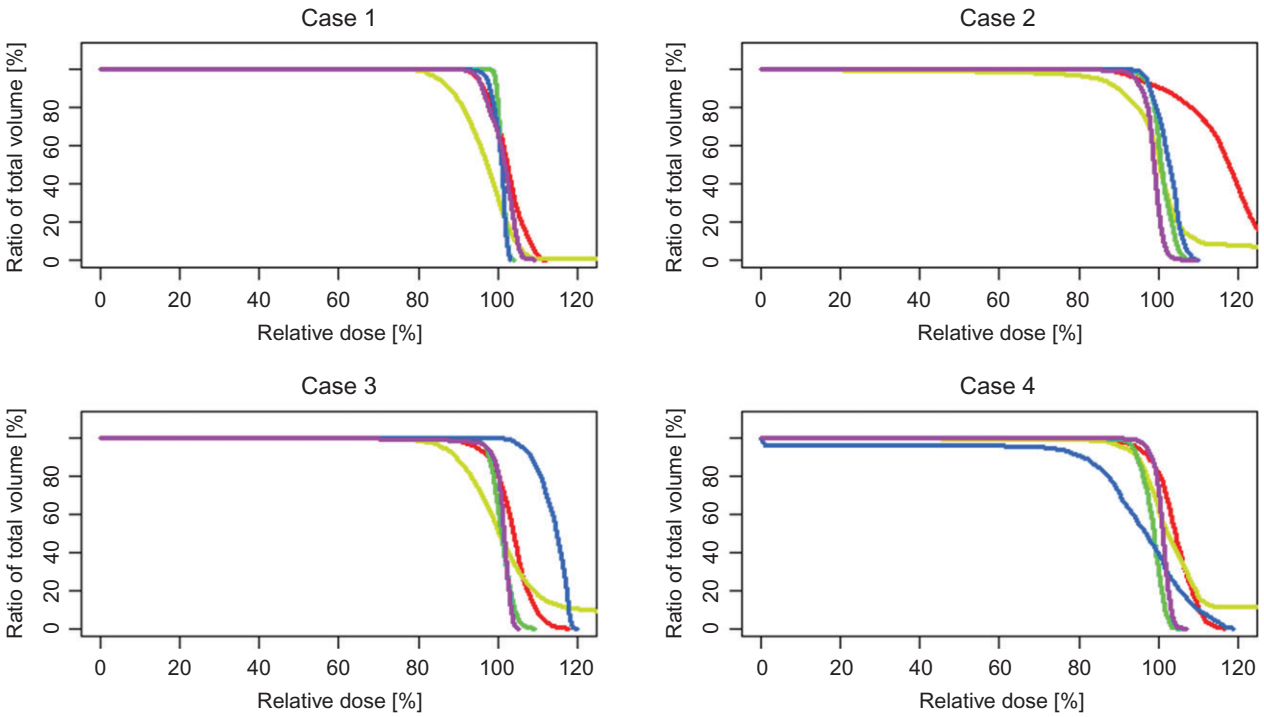

Fig. 5. Planning target volume (PTV) dose–volume histogram (DVH) profiles by modality. Plotted are DVHs showing PTV coverage for Case 1: retro-orbital melanoma; Case 2: large squamous cell carcinoma over superior eyelid; Case 3: medial canthus lesion number 1; and Case 4: second medial canthus lesion. Red, orange, green, blue and magenta colors correspond to plans for electron therapy, electrons with orthovoltage bump, volumetric-modulated arc therapy, conformal arc therapy and proton therapy, respectively.

technique (electrons, OBE), there was no depth-related positioning error; therefore, PTV expansion along the axis of the beam could either be ignored or reduced to 1–2 mm, thus improving coverage statistics drastically. This is in contrast to the VMAT and conformal arc techniques, in which accurate localization in all axes is required.

In every case, protons offered excellent coverage, homogeneity, and OAR sparing. However, the OBE technique showed promise for optimal dose distributions in very specific cases—periocular tumors extending ≤4 cm, where geometric sparing is more important than dose conformity to the target. Since accessibility to protons is still geographically and financially restricted, OBE may be an economical alternative with good retinal sparing in these select cases.

Given the simplicity of combining electrons and orthovoltage, their lower cost, their relatively widespread availability compared with protons, and the ease of planning and clinical mark-ups, our proposed novel technique (OBE) may have a role in treating facial lesions that extend deep or are in positions where direct apposition of bolus is difficult, such as the medial canthus. While we only review a limited number of cases and profiles, this study was sufficient to provide proof of concept for considering the technique in select difficult cases. While not appropriate for all periocular lesions (Cases 1 and 2) there was a dosimetric advantage for lesions extending ≤4 cm along the medial canthus when proton therapy is unavailable.

On reviewing the homogeneity, both electron treatments and conformal arc therapy were noted to have significant hotspots at 120%. As expected, proton therapy plans had excellent coverage and rapid fall-off. In OBE plans, a tail of >120% of the prescribed dose was due to the high orthovoltage dose in bone, where the f-factor is 3–4 due to the photoelectric effect [25]. No plan showed unacceptable coverage; however, when using electrons alone, the PTV V120% for Case 2 was deemed unacceptable. This did not change significantly when increasing the energy to 16 MeV, but d_{max} could be lowered to 110% by repositioning bolus to below the mask (an unrealistic clinical scenario).

When considering PDDs across modalities, it is important to note that all profiles were calculated as the patient would be treated, with or without bolus. Dose profiles were chosen to start at the body surface, below any bolus used, and to run through the GTV perpendicular to body surface. Hence, in these cases, caution must be employed when comparing conformal arc plans, VMAT plans, and two-beam proton plans with plans using single-beam modalities (electrons and OBE). For example, $De_{30\%}$ was similar between VMAT, electron only, and OBE plans, but the 30% isodose lines splayed out laterally in the VMAT plans and not in the electron or OBE plans. This was expected, but not often intuitive [1, 4, 26]. What was perhaps more enlightening was the flat dose profiles of protons across all cases. No other single modality was able to achieve this. Also of note, the PDD for Case 2 exemplified an

Table 2. Dose–volume histogram data

Structure	Metric	Electrons	OBE	VMAT	Conf arcs	Protons
Case 1						
PTV	$V_{90\%}$	100	85.0	100	100	100
	$V_{95\%}$	100	61.6	100	99.5	95.8
Retina	$V_{80\%}$	82.6	52.7	35.3	25.4	27.0
Optic nerve	$V_{100\%}$	NA	NA	NA	NA	NA
Case 2						
PTV	$V_{90\%}$	98.7	90.2	100	100	99.6
	$V_{95\%}$	95.0	79.1	98.0	99.5	96.2
Retina	$V_{80\%}$	100.0	79.4	98.9	87.2	100.0
Optic nerve	$V_{100\%}$	19.4	2.1	1.4	4.2	0.6
Case 3						
PTV	$V_{90\%}$	98.7	89.5	100	100	98.0
	$V_{95\%}$	95.0	73.1	99.3	100	97.9
Retina	$V_{80\%}$	91.3	36.5	56.9	52.4	43.7
Optic nerve	$V_{100\%}$	36.9	0	0	0.3	0
Case 4						
PTV	$V_{90\%}$	98.6	96.8	99.7	71.4	100
	$V_{95\%}$	95.0	88.4	87.9	55.6	98.7
Retina	$V_{80\%}$	42.6	33.4	38.7	18.3	48.3
Optic nerve	$V_{100\%}$	0	1.0	0	0	0.9

Values $V_{x\%}$ are the values as percentages (%) of the prescribed dose received by x% of the volume (i.e. $V_{90\%}$ of 98.7 means 98.7% of the structure's volume received 90% of the prescribed dose).

expected spike in dose for the OBE case at 2.5 cm as the beam traversed the sphenoid bone and the photoelectric effect became the dominant dose-depositing interaction.

Despite the comprehensive nature of the comparisons used and the care taken to ensure comparisons were equivalent, there are several limitations to this study. First, since calculating kilovolt dose distributions is a time-intensive process, only four cases were examined to establish a proof of principle. Investigation over a larger number of patients will be necessary in order to obtain more conclusive statistics before one technique can be declared superior to another. Second, comparing the techniques necessitated calculating dose distributions using five different dose algorithms—Eclipse Monte Carlo (electrons, protons), Eclipse AAA (VMAT), BrainScan (conformal arcs), and kVDoseCalc (OBE). This is an unavoidable limitation since no treatment-planning software that models the entire range of physics necessary to compare these entirely different radiation delivery mechanisms exists. Additionally, the use of different treatment-planning software causes technical problems. For example, Eclipse exports dose distributions in standard DICOM format in planes 2 mm apart (regardless of the dose calculation resolution.); this meant that patients with 1 mm slice datasets required interpolation to create sum OBE plans. Furthermore, kVDoseCalc calculates the dose to discrete voxels, while BrainScan and Eclipse calculate the dose in arbitrary geometrical grids.

While these technical limitations are extremely challenging to quantify perfectly, they only affect the calculation of dose on a scale of the submillimeter, which only affects the accuracy near the dose gradients. However, the structures for which we evaluated the DVH are formed of thousands to hundreds of thousands of pixels, the majority of which are located in a low-gradient dose region. Therefore, while the exact value of the dose in individual pixels, or of a certain DVH metric could be affected by submillimeter averaging errors being handled differently by the different treatment

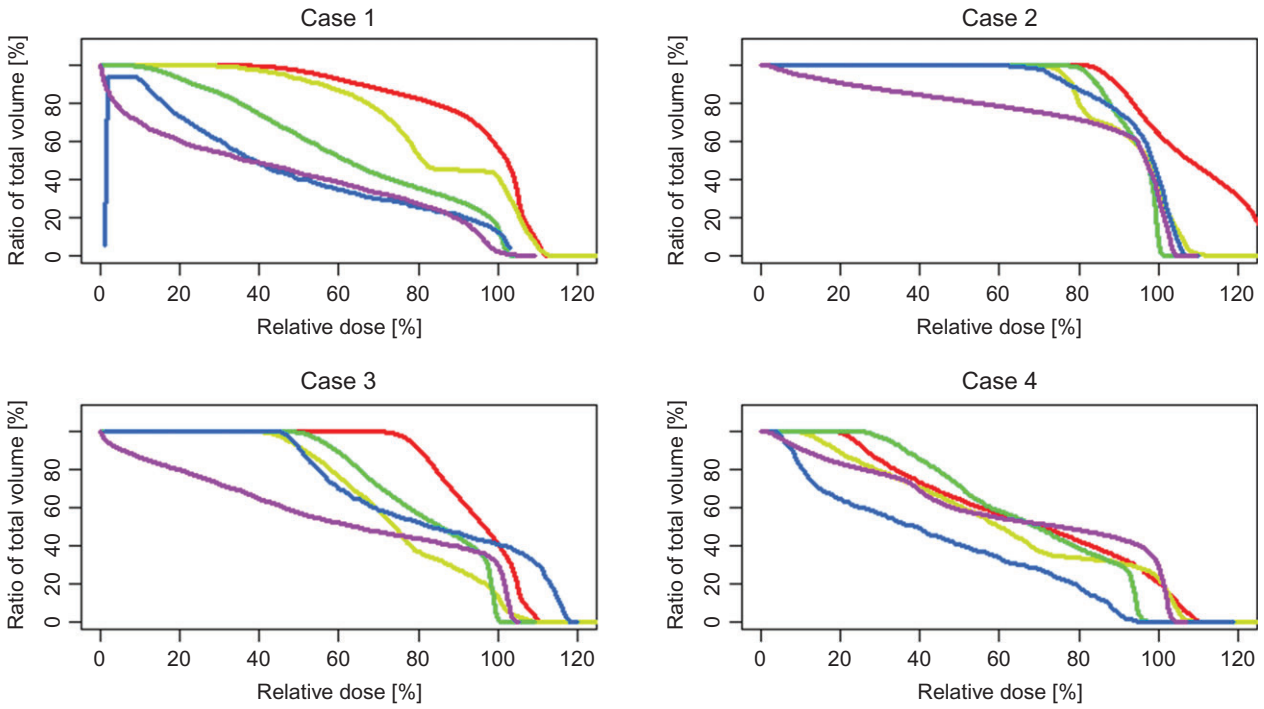

Fig. 6. Retinal dose–volume histogram (DVH) profiles by modality. Plotted are DVHs showing retinal dose for Case 1: retro-orbital melanoma; Case 2: large squamous cell carcinoma over superior eyelid; Case 3: medial canthus lesion number 1; and Case 4: second medial canthus lesion. Red, orange, green, blue and magenta colors correspond to plans for electron therapy, electrons with orthovoltage bump, volumetric-modulated arc therapy, conformal arc therapy and proton therapy, respectively.

planning systems, the broad conclusions of this study are highly unlikely to be affected.

Furthermore, we did not assess the dosimetric effect of the uncertainty in eye shield placement. Additionally, although we did see improved geometric sparing in OBE cases over electrons alone, it is unclear whether improved dosimetry would lead to superior clinical outcomes. Comparisons between OAR constraints and target coverage were also oversimplified, as radiobiologic effectiveness across modalities was not accounted for. Finally, we did not discuss the utility of surgical excision or Moh's micrographic surgery due to the risk of enucleation or large deforming defects in these sites [11, 27].

Due to the much sharper penumbras of kilovolt X-ray beams compared with electrons, in principle, it is possible to achieve the required OBE technique by using a smaller aperture for the kilovolt field compared with that of the electron. Although we were able to show the potential for our novel OBE technique for achieving geometric sparing of OARs, we did not complete a sensitivity analysis of the ideal kilovolt aperture for varying sizes of electron fields. Therefore, further optimization may be possible to create even more superior dose distributions.

This work represents the first description and proof of concept of a novel combined orthovoltage – electron radiation therapy technique. We compared dose distributions for our proposed technique with those of conventional radiotherapy techniques for four difficult-to-treat periorbital tumor cases. While inadequate for two of the cases with deep or large lesions, the proposed technique showed potential in the other two cases, where this technique might be beneficial for medial canthus lesions given its simplicity and the widespread availability of both electron and orthovoltage therapy.

SUPPLEMENTARY DATA

Supplementary data are available at *Journal of Radiation Research* online.

ACKNOWLEDGEMENTS

The authors would like to thank Eduardo Villarreal-Barajas and Laurel Traptow for their advice, help and support on this project. Some of the results of this study were presented at the American Association of Physicists in Medicine annual meeting 2017 and at the Canadian Association for Radiation Oncology annual meeting 2016.

CONFLICT OF INTEREST

The authors have no competing interests to disclose

FUNDING

This research is supported by departmental funding in the Department of Oncology at the University of Calgary.

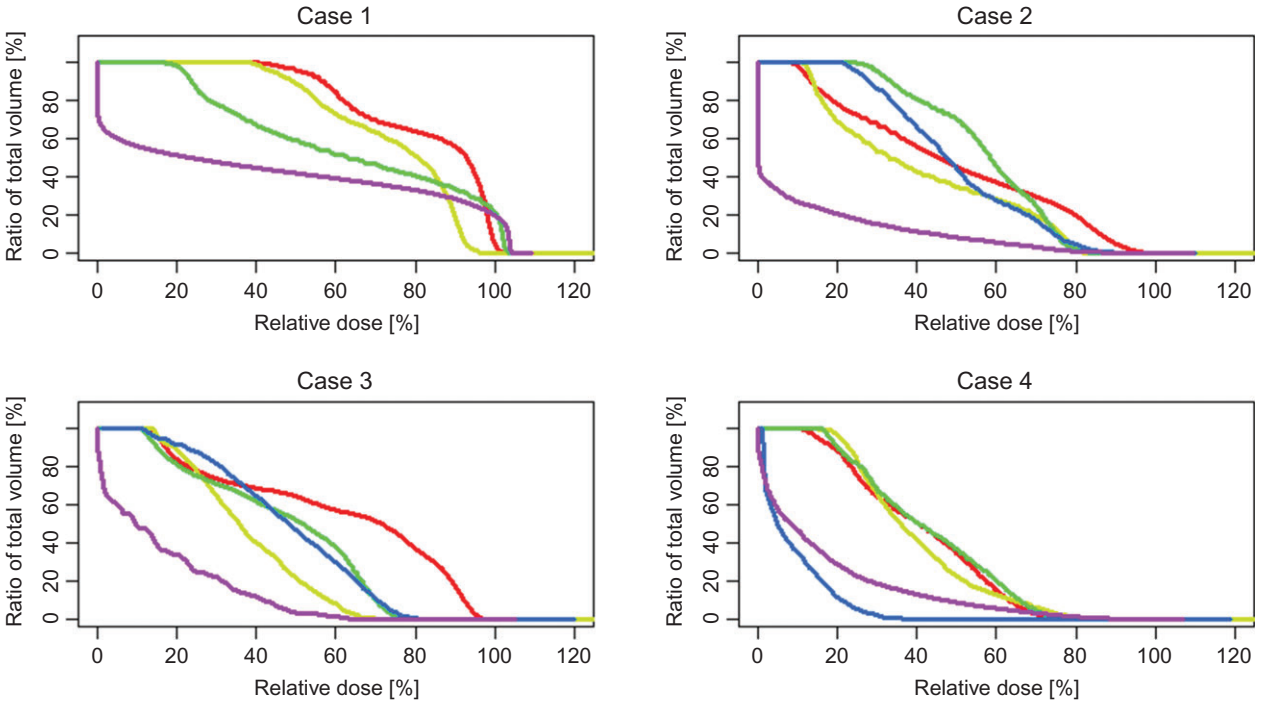

Fig. 7. Ipsilateral optic nerve dose–voume histogram (DVH) profiles by modality. Plotted are DVHs showing ipsilateral optic nerve dose for Case 1: retro-orbital melanoma; Case 2: large squamous cell carcinoma over superior eyelid; Case 3: medial canthus lesion number 1; and Case 4: second medial canthus lesion. Red, orange, green, blue and magenta colors correspond to plans for electron therapy, electrons with orthovoltage bump, volumetric-modulated arc therapy, conformal arc therapy and proton therapy, respectively. Of note, optic nerve sparing would not normally be prioritized in Case 1.

REFERENCES

1. Khan F. Electron beam therapy. In: Khan F (ed). *The Physics of Radiation Therapy*, 4th edn. Philadelphia, PA: Lippincott Williams & Wilkins, 2010, 272–74.
2. Shiu AS, Tung SS, Gastorf RJ et al. Dosimetric evaluation of lead and tungsten eye shields in electron beam treatment. *Int J Radiat Oncol Biol Phys* 1996;35:599–604.
3. St. Aubin J, Villarreal-Barajas J, Newcomb C. SU-E-T-326: Investigating the use of tantalum mesh bolus in electron beams. *Med Phys* 2011;38:3562.
4. Teoh M, Clark CH, Wood K et al. Volumetric modulated arc therapy: a review of current literature and clinical use in practice. *Br J Radiol* 2011;84:967–96.
5. Frank SJ, Selek U. Proton beam radiation therapy for head and neck malignancies. *Curr Oncol Rep* 2010;12:202–7.
6. Holliday EB, Frank SJ. Proton radiation therapy for head and neck cancer: a review of the clinical experience to date. *Int J Radiat Oncol Biol Phys* 2014;89:292–302.
7. Kasper ME, Chaudhary AA. Novel treatment options for non-melanoma skin cancer: focus on electronic brachytherapy. *Med Devices* 2015;8:493–502.
8. Stannard C, Sauerwein W, Maree G et al. Radiotherapy for ocular tumours. *Eye* 2013;27:119–27.
9. Lievens Y, Pijls-Johannesma M. Health economic controversy and cost-effectiveness of proton therapy. *Semin Radiat Oncol* 2013;23:134–41.
10. Das I, Gillin M, Galvin J et al. *ACR-AAPM technical standard for the performance of proton beam radiation therapy*, Vol. 1076. Technical Standard. ACR-AAPM, 2013. https://www.acr.org/-/media/ACR/Files/Practice-Parameters/proton-therapy-ts.pdf?la=en (3 November 2017, date last accessed).
11. Mohs FE. Micrographic surgery for the microscopically controlled excision of eyelid cancer: history and development. *Adv Ophthalmic Plast Reconstr Surg* 1986;5:381–408.
12. Haddad P, Cheung F, Pond G et al. Computerized tomographic simulation compared with clinical mark-up in palliative radiotherapy: a prospective study. *Int J Radiat Oncol Biol Phys* 2006;65:824–9.
13. D'Alimonte L, Sinclair E, Seed S. Orthovoltage energies for palliative care in the 21st century: Is there a need? *Radiography* 2011;17:84–7.
14. Brouwer CL, Steenbakkers RJHM, Bourhis J et al. CT-based delineation of organs at risk in the head and neck region: DAHANCA, EORTC, GORTEC, HKNPCSG, NCIC CTG, NCRI, NRG Oncology and TROG consensus guidelines. *Radiother Oncol* 2015;117:83–90.
15. Thomas SJ. Margins between clinical target volume and planning target volume for electron beam therapy. *Br J Radiol* 2006;79:244–7.

16. Sommerville M, Poirier Y, Tambasco M. A measurement-based X-ray source model characterization for CT dosimetry computations. *J Appl Clin Med Phys* 2015;16:5231.
17. Kouznetsov A, Tambasco M. A hybrid approach for rapid, accurate, and direct kilovoltage radiation dose calculations in CT voxel space. *Med Phys* 2011;38:1378–88.
18. Grafe J, Poirier Y, Jacso F et al. Assessing the deviation from the inverse square law for orthovoltage beams with closed-ended applicators. *J Appl Clin Med Phys* 2014;15:4893.
19. Poirier Y, Kouznetsov A, Koger B et al. Experimental validation of a kilovoltage x-ray source model for computing imaging dose. *Med Phys* 2014;41:41915.
20. Hagen B, O'Beirne M, Desai S et al. Innovations in the ethical review of health-related quality improvement and research: The Alberta Research Ethics Community Consensus Initiative (ARECCI). *Healthc Policy* 2007;2:e164–77.
21. Johnstone CD, Lafontaine R, Poirier Y. Modeling a superficial radiotherapy X-ray source for relative dose calculations. *J Appl Clin Med Phys* 2015;16:118–30.
22. Poirier Y, Tambasco M. Experimental validation of a kV source model and dose computation method for CBCT imaging in an anthropomorphic phantom. *J Appl Clin Med Phys* 2016;17:155–71.
23. Poludniowski G, Landry G, DeBlois F et al. SpekCalc: a program to calculate photon spectra from tungsten anode x-ray tubes. *Phys Med Biol* 2009;54:N433–8.
24. Emami B, Lyman J, Brown A et al. Tolerance of normal tissue to therapeutic irradiation. *Int J Radiat Oncol Biol Phys* 1991;21:109–22.
25. Seuntjens J, Thierens H, Van der Plaetsen A et al. Conversion factor f for X-ray beam qualities, specified by peak tube potential and HVL value. *Phys Med Biol* 1987;32:595–603.
26. Tailor RC, Hanson WF. Calculated absorbed-dose ratios, TG51/TG21, for most widely used cylindrical and parallel-plate ion chambers over a range of photon and electron energies. *Med Phys* 2002;29:1464–72.
27. Mohs FE. Chemosurgery for the microscopically controlled excision of cutaneous cancer. *Head Neck Surg* 1978;1:150–66.